J Neurol Disord
Volume 10:2, 2022

Journal of Neurological Disorders

Review

Open Access

Sirt1 Mediated High-Glucose Induced Aβ Deposition and Cognitive Impairment through Activation of the TLR9/P53 Pathway

Yue Sun[1], Shiyu Zhu[1], Jinliang Chen[1], Yuxing Zhao[1], Cheng Luo[1], Lv Qiong[1], Zhiyin Liao[1], Kexiang Zhao[1], Yuan Gao[1], Di Wang[2] and Qian Xiao[1*]

[1]Department of Emergency and Intensive Care Medicine, Chongqing Medical University, Chongqing, China
[2]Department of Emergency and Intensive Care Medicine, AMU (SOUTHWEST HOSPITAL), Chongqing, China

Abstract

Aim: DE is a chronic central nervous system complication caused by DM. Aβ² deposition has been considered as the main cause of cognitive impairment in DE. Our study explored the function of non-inflammatory pathway of TLR9, that acting on Sirt1 related Aβ² deposition and cognitive function in DE.

Methods: Wide type and TLR9 knockout C57BL/6J mice were randomly divided into a control and a DM group. The DM rat was produced by intraperitoneal injection of STZ. And adeno associated virus was injected into their hippocampi to inhibit Sirt1. 12 weeks later, the rats were tested in water maze and then sacrificed. Hippocampi were for immunohistochemistry, Western blot, and RT-PCR. *In vitro* HT22 cells were incubated with or without high glucose medium and further intervened with TLR9 antagonist ODN2088 and p53 over expressed lent viral infection. The detection method was almost the same as *in vivo*, except for flow cytometry.

Results: We found that, compared with DM mice, TLR9-/-DM mice performed better in learning ability and short term memory and contained lower Aβ², but could be reversed by Sirt1 inhibition. Furthermore, *in vitro*, after intervention with high glucose and p53 over expressed lentiviral infection, we observed the positive results of TLR9 inhibition, such as Sirt1 up regulation, Aβ² reduction or cognitive improvement, were reversed (all $P<0.05$).

Conclusion: We considered that TLR9/p53/Sirt1 signalling pathway induced by high glucose are one of molecular mechanisms underlying DE. These results not only confirm the importance of blood glucose management but also provide new insights for treatment of DE.

Keywords: Neurology • Inhibition • Nervous system

Introduction

Diabetes mellitus (DM) is a metabolic disease with main clinical characteristics of hyperglycemia and insulin resistance. Diabetic encephalopathy (DE), as the central nervous complication of DM, was initially described by Nielsen and found diffuse degeneration, fibrotic changes of the pia mater, and cerebral atherosclerosis in cerebral cortex and dentate nucleus [1].

Further pathophysiological studies showed that DE is similar with Alzheimer's disease (AD) for the two major features senile plaques (SPs) or neurofibrillary tangles (NFTs), and glucose metabolic disorder or insulin resistance [2-4]. Epidemiological analyses have enhanced the connection between DE and AD for the reason that DM is one of the most common comorbidities of almost all the sporadic AD [2]. Despite being partially overlapped with characters of AD and regarded as "brain type DM", the underlying pathogenic mechanism of DE is still worth debating.

As the main component of neuritic plaques, β-amyloid peptide (Aβ) is a recognized neurotoxin Aβ, especially Aβ40 and Aβ42, being proved to activate inflammatory responses through proliferation of glial cells, which participates in the loss of neuronal synapses in the brain. Previous studies, including ours, indicate that DM will promote Aβ deposition in the hippocampus to influence cognitive function, which shows the possibility of Aβ in development and potential treatment of DE [5-7].

Silent information regulator 1 (Sirt1) is a nicotinamide adenine dinucleotide dependent histone deacetylase which might connect excessive Aβ deposition with cognitive dysfunction of DM. Previous studies showed that down expression of Sirt1 contributes to some chronic complications of DM, such as diabetic peripheral neuropathy and diabetic nephropathy. Recently studies confirmed that Sirt1 could alleviate Aβ deposition in brain and improved cognitive functions of AD patients or mice, providing a hint that Sirt1 might play a vital role to deal with excessive Aβ deposition of DE [8-10]. In our research we have proved that high glucose induced reduction of Sirt1 is responsible for excessive deposition of Aβ in hippocampus through activating ADAM10 and suppressing BACE1. Further *in vivo* we observed that knocking out TLR9 (TLR9 KO) could improve the cognitive functions of DM mice, attenuate Aβ deposition in their brain, and reverse the inhibitory state of Sirt1. However, the effects were offset when selectively down regulating Sirt1 by injecting AAV (adeno associated virus) in hippocampi, indicating that TLR9 participated in regulating Sirt1 in DE. We also found that p53, being up regulated by TLR9, could suppress Sirt1 [11]. To summarize these results show that high glucose induced cognitive impairment and Aβ deposition are mediated by TLR9/p53/Sirt1 signalling pathway.

Effect of TLR9 KO and Sirt1-AAV treatments on cognitive impairment in mice with STZ induced diabetes. Morris water maze were used to elevate the cognitive function of all mice. Acquisition trial lasted for five days with the hidden platform, following a probe trial with the hidden platform and a visible trial with the visible platform (Figure 1).

***Address for Correspondence:** Qian Xiao, Department of Geriatrics, The First Affiliated Hospital of Chongqing Medical University, Chongqing 400016, China Email: xiaoqian1956@126.com*

Received: 02-Feb-2022, Manuscript No. jnd-22-54008; **Editor assigned:** 04-Feb-2022, Pre QC No: P-54008 (PQ); **Reviewed:** 18 Feb-2022, QC No. Q-54008; **Revised:** 23 Feb-2022, Manuscript No. R-54008; **Published:** 02- March-2022, **DOI no:** 10.4172/2329-6895.10.2.479.

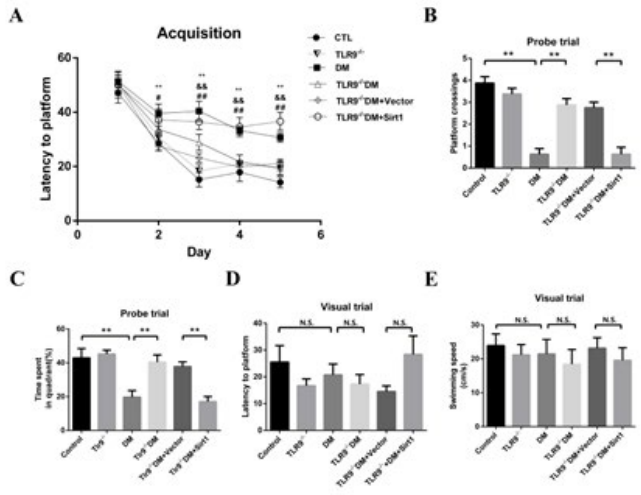

Figure 1. (A) The trend about the escape latency of each group to find the hidden platform during five consecutive days of the acquisition trial. Data were analyzed using a two-way ANOVA of repeated measures followed by Tukey's post hoc tests. **P<0.01 represents DM group vs. control group. &&P<0.01 represent DM group vs. TLR9-/-DM group. #P<0.5 and ##P<0.01 represent TLR9-/-DM+Vector group vs. TLR9-/-DM+Sirt1 group. (B) Number of platform crossings and (C) percentage of time spent in the target quadrant during the probe trial. (D) Latency to reaching the platform and (E) swimming speed during the visual trial. Data were analyzed using a one-way ANOVA followed by Tukey's post hoc tests. *P<0.05, **P<0.01. Results were expressed as mean ± SEM (n=8 animals a group).

Methods

Animals

Three week old TLR9 KO transgenic mice (C57BL/6J-Tlr9M7Btlr/Mmjax, 014534) were purchased from the Jackson Laboratory (JAX, USA). Other age matched experimental mice（C57BL/6J）were purchased from the Animal Centre of Chongqing Medical University, China. All mice were propagated and housed in the Animal Centre of Chongqing Medical University. Breeding mice were housed at 3 per cage (2 females and 1 male), and experimental mice were housed at 5 mice (all males) per cage in the IVC system. During the housing period, the environmental temperature was 22 ± 2°C, and a 12 h day/night cycle was ensured (lights on 8 am-8 pm). Sufficient food and water were supplied.

Experimental protocols

Eight week old wild type (n=16) and TLR9-/-mice (n=32) with a mean body weight of approximately 24 g were randomly divided into the following 6 groups: (1) Control group, (2) TLR9-/-group, (3) DM group, (4) TLR9-/-DM group, (5) TLR9-/-DM+Vector group, and (6) TLR9-/-DM+Sirt1 group. STZ was purchased from Sigma-Aldrich Co. (St. Louis, MO, USA), and the m-Sirt1 AAV (HBAAV2/9-U6-sirt1 gRNA8-cas9, gRNA8: CCGTCTCTTGATCTGAAGTC) and vector (HBAAV2/9-GFP), were purchased from HANBIO Technology Co. Ltd. (Shanghai, China). After 1 week of adaptation, the mice in the DM, TLR9-/-DM, TLR9-/-DM+Vector, and TLR9-/-DM+Sirt1 groups were injected with STZ (TLR9 KO mice, 130 mg/kg; normal mice, 180 mg/kg) dissolved in 0.1 M sodium citrate buffer (pH 4.4) using an i.p. injection to establish the type 1 DM model. Three days after the STZ injection, the fasting blood glucose was monitored; when the level was above 16.67 mmol/L, the DM model was considered to be established successfully. Next, non-fasted blood glucose levels were monitored randomly at weeks 4, 8, and 12 through the mouse tail vein. At 4 weeks after STZ injection, the bilateral hippocampi of the mice in the TLR9-/-DM+Vector and TLR9-/-DM+Sirt1 groups were injected with the vector (3 μL per side; viral titre 1012 v.g./mL) and the Sirt1 AAV (3 μL per side; viral titre 1012 v.g./mL), respectively, using a stereotaxic frame (Stoelting Co., Ltd., USA), to selectively inhibit hippocampal Sirt1 expression.

Water maze experiment

To measure the differences in the learning and cognitive abilities of the mice, a 6-d Morris water maze (MWM) test was performed at 12th week after STZ injection. The water maze instrument (130 cm diameter and 50 cm height) was divided into 4 quadrants. The depth of the water was 30 cm, and the water temperature was maintained at 22 ± 1°C. The platform (10 cm diameter) was placed in the target quadrant and was lower than the water level by approximately 1 cm-2 cm; the location was not changed. The experimental mice received 4 training sessions every day for 5 days. At the beginning of each training session, the mice were randomly placed in one of the 4 quadrants (head facing the pool wall). The training was stopped when the mice found the platform or the exploration time reached the time limit of 90's, after which the technician led the mice to the platform within 15's. After 5 day training was finished, the differences in escape latency were analysed to evaluate the spatial learning ability of the experimental mice. The exploratory experiment was performed within 24 h of the completion of the training. The platform was removed, and the mice were allowed to swim for 90's. The time period required by each mouse to find the target quadrant in which the platform was originally placed and the number of times they entered this quadrant were recorded as the indicators for evaluating the spatial memory ability.

After the exploratory experiment, the visible platform test was performed to exclude the influences of differences in vision and muscle strength on the accuracy of the water maze experiment. This procedure raised the platform such that it was higher than the water level by 1 cm. The mice could see the platform during the swimming process. The parameters recorded were the time required for the mice to climb on the platform and the swimming speed of the mice.

Tissue preparation

Following behavioural testing, all mice were deeply anaesthetised using 1% pentobarbital sodium (40 mg/kg) at 21 weeks of age. The bilateral hippocampi were removed and immediately placed in liquid nitrogen for future western blotting (WB). For immunohistochemistry (IHC), mice were perfused with 0.9% saline transcardially followed by 4% paraformaldehyde (PFA). Brains were removed and fixed in 4% PFA at 4°C.

Cell culture and intervention

The neuronal cell line HT22 was obtained from the ATGG cell bank. All procedures for the cell experiments were performed using sterile technique in order to avoid microbial contamination. The cell culture environment was a cell culture incubator (under 5% CO2 at 37°C). The HT22 cells were cultured in high glucose Dulbecco's modified Eagle's medium (H-DMEM, Gibco BRL Co, Ltd., USA) containing 10% foetal bovine serum (FBS, Gibco BRL Co, Ltd., USA). Cells were passaged (at ratios of 1:3-4) when the cell confluence reached approximately 80%. Adherent cells were digested using 0.25% trypsin without EDTA (Gibco BRL Co, Ltd., USA) for approximately 3-5 minutes, collected, and centrifuged. After the supernatant was discarded, the cells were placed in new cell culture flasks. Some cells were collected in dimethyl sulfoxide (DMSO, Thermo Scientific, Waltham, MA, USA) cryopreservation solution and stored in liquid nitrogen. The cells were treated for 3 days with 25 mM glucose (yielding a total glucose concentration of 50 mM) or 25 mM mannitol, which was used as an osmotic control [12]. To regulate the expression of TLR9 and wild type p53, the cells were pre-treated with the TLR9 antagonist ODN2088 (ODN; 5 μM, InvivoGen, Thermo Fisher Scientific Inc., Waltham, USA) and sh-p53 [rLV-mP53-ZsGreen-Puro, mouse wild type P53 (NM_011640), viral titre 108 TU/mL, Labcell Inc., Chongqing, China].

Western blotting

Hippocampal tissues from the mice were homogenized in radio immune precipitation assay buffer (RIPA buffer, Beyotime Inc. Shanghai, China)

containing a protease and phosphatase inhibitor cocktail (Roche, Switzerland). The protein concentration was measured using the bicinchoninic acid assay (BCA assay kit, Beyotime Inc. Shanghai, China). All protein samples were adjusted to the same concentration. After thorough mixing, the samples were loaded for protein separation. A 10-12% SDS-polyacrylamide gel was used as the separating gel. The voltage was 100 V, and the electrophoresis time was 120 min. After the electrophoresis was finished, the separated proteins were transferred to a polyvinylidene difluoride (PVDF, Millipore, Dundee, Scotland, UK) membrane. The membrane was immediately blocked in a 5% bovine serum albumin (BSA) solution at room temperature for 1 h. Primary antibodies targeting the following proteins were used: TLR9 (1:500, Imgenex, Novus, USA, IMG-305A), Sirt1 (1:500, Imgenex, Novus, USA, 51641), Phospho-P38MAPK (1:1000, Cell Signaling Technology Co. Ltd., Massachusetts, US, 8690), total P38MAPK (1:1000, Cell Signaling Technology Co. Ltd., Massachusetts, US, 8690), p53 (1:500, Abcam Co. Ltd., Cambridge, UK, ab26), ADAM10 (1:1000, Abcam Co. Ltd., Cambridge, UK, 124695), BACE1 (1:500, Abcam Co. Ltd., Cambridge, UK, 108394), LC3B (1:1000, Abcam Co. Ltd., Cambridge, UK, 192890), Atg5 (Cell Signaling Technology Co. Ltd., Massachusetts, US, 12994), P62 (Cell Signaling Technology Co. Ltd., Massachusetts, US, 23214), Beclin1 (Cell Signaling Technology Co. Ltd., Massachusetts, US, 3495), Aβ (1:500, Imgenex, Novus, USA, NBP2-13075), Aβ40 (1:500, Synaptic Systems Co. Ltd, Germany, 218221), Aβ42 (1:500, Synaptic Systems Co. Ltd, Germany, 218721), Caspase 3 (1:1000, Gene Tex, Inc., California, USA, GTX110543), Pro-caspase 3 (1:500, Abcam Co. Ltd., Cambridge, UK, ab32150) and β-actin (1:1000, Zhongshan Inc. Beijing, China). Primary antibodies were incubated with the membrane at 4°C overnight. On the following day, the membrane was rinsed 3 times in Tris-buffered saline-Tween 20 solution. Then, the membrane was incubated with the corresponding horseradish peroxidase labelled secondary antibody（1：100，Zhongshan Inc. Beijing, China at 37°C for 1 h. The membrane was rinsed 3 times in TBST, and an enhanced chemiluminescence reagent (Thermo Scientific, Waltham, MA, USA) was added to develop the target proteins. The greyscale density of the protein band was analysed using substrateBio-1D software (Vilber Lourmat, Marne-la-Vallée, France).

Immunohistochemistry

Brains were fixed in 4% PFA for 24 h after having been dissected out. Then they were embedded in paraffin, and tissue sections (4-6 μm) were obtained for IHC analysis. For heat induced epitope retrieval, deparaffinized and hydrated sections were incubated in 1 mM citrate buffer (pH 6.0) at 95°C for 30 min in a microwave oven. Then sections were incubated with 3% H2O2 for 20 min. Nonspecific binding was blocked via incubation with 10% goat serum for 30 min at 37°C. After that sections were treated with the primary antibody of Aβ (1:200, Imgenex, Novus, USA, NBP2-13075) overnight at 4°C. After washing with PBS, sections were incubated with biotinylated secondary antibody (Zhongshan Inc. Beijing, China) for 30 min at 37°C. Finally immuno reactivity were detected by diaminobenzidine. Sections were dehydrated and mounted on slides. All sections were blindly examined with the microscope at ×40×100×400 magnification.

Flow cytometric analysis

After interventions with high glucose, TLR9 inhibitors or lentiviral infection, the apoptotic rates in all groups of HT22 cells were evaluated following the protocol of Annexin V-FITC Apoptosis Detection Kit (Vazyme Biotech Co., Ltd, A211). The adherent cells were digested for 3 minutes and then were centrifuged twice. After incubation with Annexin V-FITC and PI staining solution for 10 minutes at room temperature, all groups were analysed via flow cytometry (BD Co. Ltd, USA).

Statistical analysis

All data were analysed using SPSS 22.0 statistical software. After the MWM experimental data were confirmed to meet the requirements of the Shapiro-Wilk test and the distribution of equal variance, the differences in the escape latency of mice on the same day among different groups were compared using two way repeated measures ANOVA, and the differences in the escape latency of mice in the same group at different time points were compared using multivariate ANOVA. The other data obtained in this study were analysed via one way ANOVA followed by Tukey's post hoc test (equal variance assumed) or Dennett's T3 post hoc test (equal variance not assumed). All data are presented as the mean ± SEM. $P<0.05$ was considered to be statistically significant.

Results

Sirt1 down regulation reversed the protective effect of TLR9 KO on cognitive function in DM mice

First, the influence of the TLR9 gene on cognitive function was investigated using the water maze paradigm. The purpose of the 5 d hidden platform experiment was to evaluate differences in the spatial learning abilities of the mice in all groups. As shown in Figure 1A, after 5 d training, the mice in all groups required less time to find the hidden platform (i.e., showed shortened escape latency), exhibiting the spatial learning ability of mice. Differences of latency among the 5 groups were compared using multivariate analysis of variance. On the first 2 training days, the latency did not show the difference. Beginning on the 3rd training day, the escape latency was significantly longer for the DM mice than for the non-DM mice, suggesting that the learning ability of the DM mice was impaired. The performance of TLR9-/-DM mice was significantly better than that of DM mice, indicating that TLR9 KO attenuated DM related cognitive dysfunction. However, this protective function was reversed after selective inhibition of hippocampal Sirt1 expression because the escape latency of TLR9-/-DM+Sirt1 mice was significantly longer than that of TLR9-/-DM+Vector mice, suggesting that Sirt1 participated in the regulation of TLR9-induced cognitive dysfunction in the DM mice.

On the 6th day of the water maze experiment, the differences in the memory ability of all the mice were evaluated using the platform withdrawal experiment. The metrics were the number of times each mouse passed through the platform area and the percentage of time it remained in the target quadrant. As shown in Figures 1B and 1C, despite the two indicators were both significantly lower in DM group, there were differences within the groups. The mice in TLR9-/-DM and TLR9-/-DM+Vector groups performed better than those in DM or TLR9-/-DM+Sirt1 group, indicating that DM damaged the short term memory function of the mice, potentially through regulation of TLR9 and Sirt1.

To exclude the influence of diabetic muscle weakness and retinopathy on the water maze results, we designed a visible platform experiment. After the platform withdrawal experiment, the platform was placed again to ensure that the mice could see and climb on the platform. As shown in Figures 1D and 1E, the 5 groups of mice did not show significant differences in escape latency in the visible platform experiment. In addition, the swimming speed did not differ among the mice. The above experimental results essentially excluded the influences of vision and muscle dysfunction in the water maze test.

Sirt1 reversed excessive Aβ deposition by activating TLR9 in hippocampi of DM mice

To ascertain the regulatory effect of TLR9 on Sirt1 and Aβ, we compared the expression of Sirt1 and Aβ *in vivo* using western blotting (WB) and IHC (Figures 2A and 3). As shown in Figures 2C and 2D, compared to the Control group, the DM group showed marked suppression of Sirt1 and increase of Aβ. The adverse function of DM on Sirt1 and the aforementioned expression of Aβ were reversed by knocking TLR9 out. These results were in accordance with that of IHC. As shown in Figure 3, we just found some neuritic plaques in the DG region of hippocampi of DM group and TLR9-/-DM+Sirt1 group. It suggested that the inverse regulation of Sirt1 by TLR9 was key to promote Aβ deposition in DM (Figures 2B and 4).

P53 was critical for Sirt1 to be regulated by the high glucose induced TLR9 activation

To concentrate on confirming the influence of pathogenic factor of DM (high glucose) on neuronal Aβ production and to identify its potential relationship between TLR9 and Sirt1, HT22 cells, the neuronal cell line, were incubated in culture medium with high glucose, TLR9 antagonist, and lentiviral over expression of p53 *in vitro*. As shown in Figure 5, compared to the Control group, the high glucose group showed higher expressions of TLR9 and p53 and hyper phosphorylation of P38, but significantly lower expression of Sirt1. After intervening with the TLR9 specific antagonist ODN2088, the trends of the above indicators were reversed, which was consistent with the results *in vivo*. What's more, we found that p53 was significantly higher in the DM mice than that in the Control or TLR9-/-DM mice, but remained same in DM+Sirt1 mice compared with DM mice, which unveiled the nonsense of Sirt1-downregulation had made on p53 (Figure 2B). However, after resuming p53 by lentiviral infection, the protective effect of TLR9 antagonist ODN2088 disappeared, resulting in re-inhibition of Sirt1 and elevation of neuronal Aβ accumulation, which suggests that wild type p53 was a key for Sirt1 to be regulated by TLR9 stimulation.

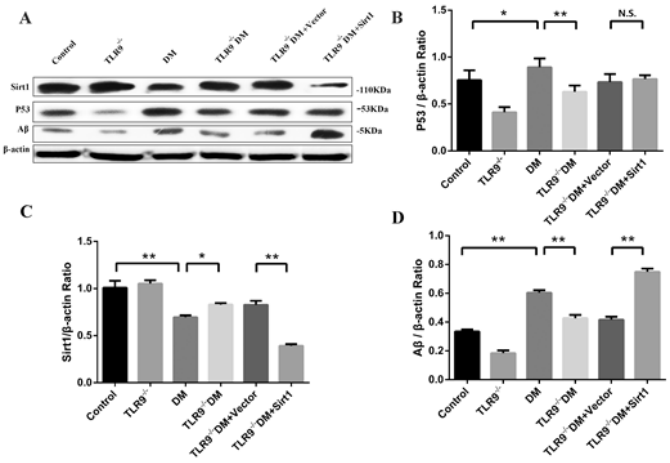

Figure 2. Effect of TLR9 KO and Sirt1-AAV treatments on Aβ deposition. (A) Western blotting of p53, Sirt1, Aβ expressions in mouse hippocampi. β-actin was used as the loading control. (B-D) Quantification of p53, Sirt1, Aβ levels . Values for the control group were arbitrarily set to a unit of 1. All data were analyzed using a one-way ANOVA followed by Tukey's post hoc tests. *P<0.05, **P<0.01, N.S., not significant. Results were expressed as mean ± SEM (n=6 animals a group).

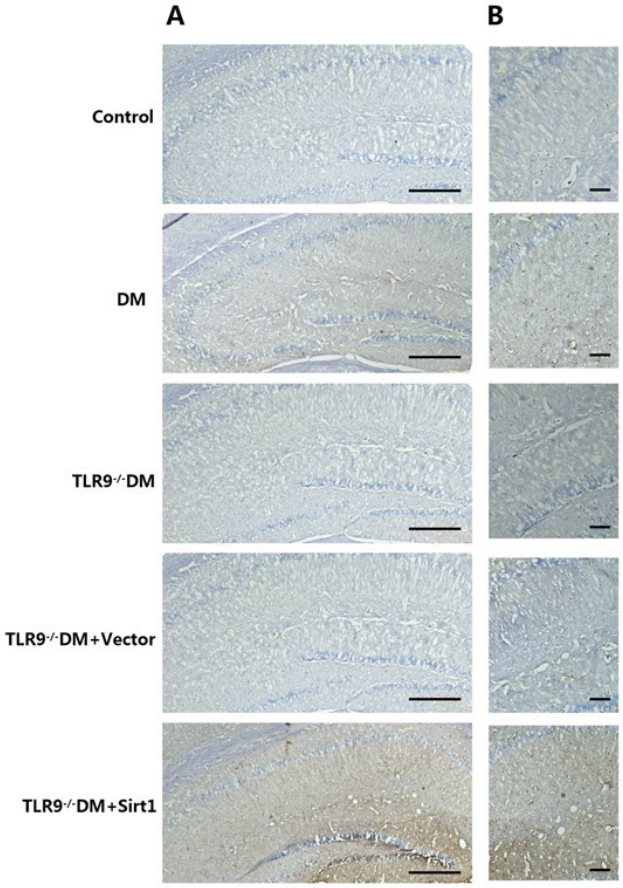

Figure 3. Effect of TLR9 KO and Sirt1-AAV treatments on Aβ expression and Neurite plaques. Immunostaining for Aβ expression and Neurite plaques in hippocampi and its dentate gyrus region（DG）. (A) Magnification ×100, scale bar=100μm. (B) Magnification ×400, scale bar=10μm.

Alterations of Sirt1-mediated β-secretase and α-secretase pathways, not the autophagy pathway, regulated by TLR9, influenced Aβ deposition in the hippocampi of DM mice

To further explore the possible signalling pathways underlying the excessive Aβ deposition in the brains of DM mice, the differences of the Sirt1-mediated expression of β-secretase 1 precursor (BACE1), a disinterring and metalloproteinase domain containing protein 10 (ADAM10), and critical proteins in autophagy pathway (Figure 4A). As shown in Figures 3B and 3C, the expression of ADAM10 was lower in the DM group than that in the Control or TLR9-/-DM groups, whereas the change of BACE1 expression was just on the contrary. When TLR9 was up regulated, the above exchange of ADAM10 and BACE1 was exactly reversed. What's more interesting, the alterative trend of Sirt1 was always consistent with ADAM10, but in contrast to BACE1. Moreover, after Sirt1 was down regulated, the Aβ metabolic pathway exhibited some changes, such as blockage of amyloid protein precursor (APP) metabolism in the α-secretase pathway and activation of the β-secretase pathway, which are accorded with tendency of ADAM10 and

BACE1 that has been revealed before, suggesting that activation of TLR9/Sirt1 signalling pathway was important for Aβ degradation in DE (Figures 4B and 4C). In addition, altered expressions of critical autophagy targets, such as increases in Beclin1, Atg5, LC3II/LC3I and a decrease in P62, were also observed in the DM group compared with the Control group. Although these alterations could be reversed in the TLR9-/-DM group, there were no differences of critical autophagy targets between the TLR9-/-DM+Vector group and the TLR9-/-DM+Sirt1 group, demonstrating that the effect of TLR9 on autophagy was dominated in DM mice, not being regulated by Sirt1 (Figures 4D-4G).

The TLR9/p53 signalling pathway participated in high glucose induced neuronal apoptosis

The results of flow cytometry showed that neuronal apoptosis significantly increased in the HG group compared with the Control group. After intervention with the TLR9 antagonist ODN2088, the rate of HT22 cells

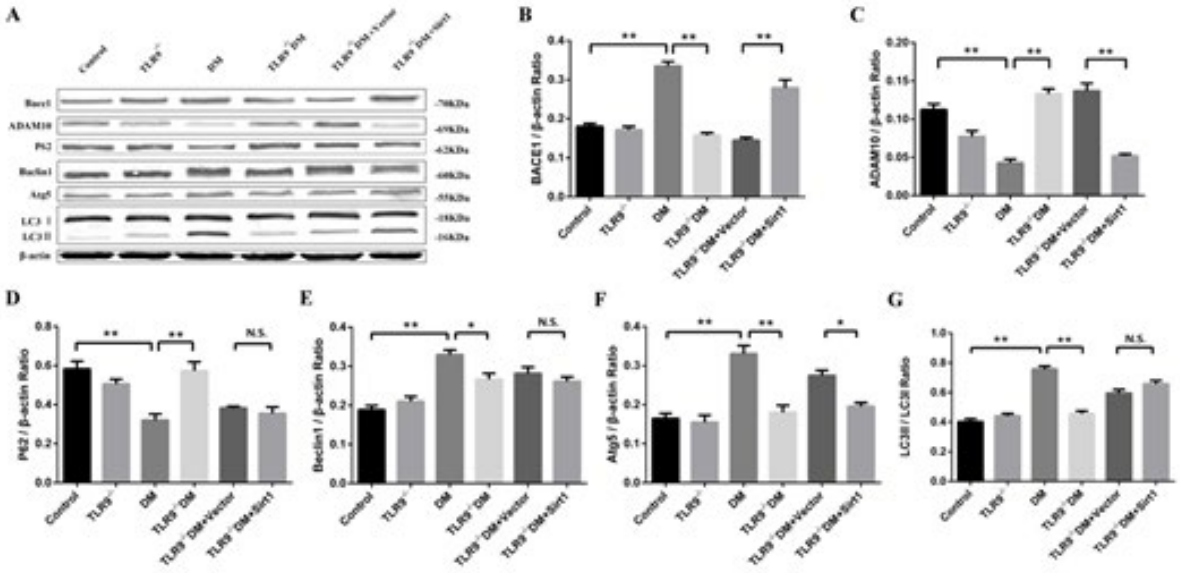

Figure 4. Effect of TLR9 KO and Sirt1-AAV treatments on key proteins in β-secretase and α-secretase and autophagy pathways. (A) Western blotting of BACE1, ADAM10, autophagy protein expressions in mouse hippocampi. β-actin was used as the loading control. (B-G) Quantification of BACE1, ADAM10, autophagy protein levels . Values for the control group were arbitrarily set to a unit of 1. All data were analyzed using a one-way ANOVA followed by Tukey's post hoc tests. *P<0.05, **P<0.01, N.S., not significant. Results were expressed as mean ± SEM (n=6 animals a group).

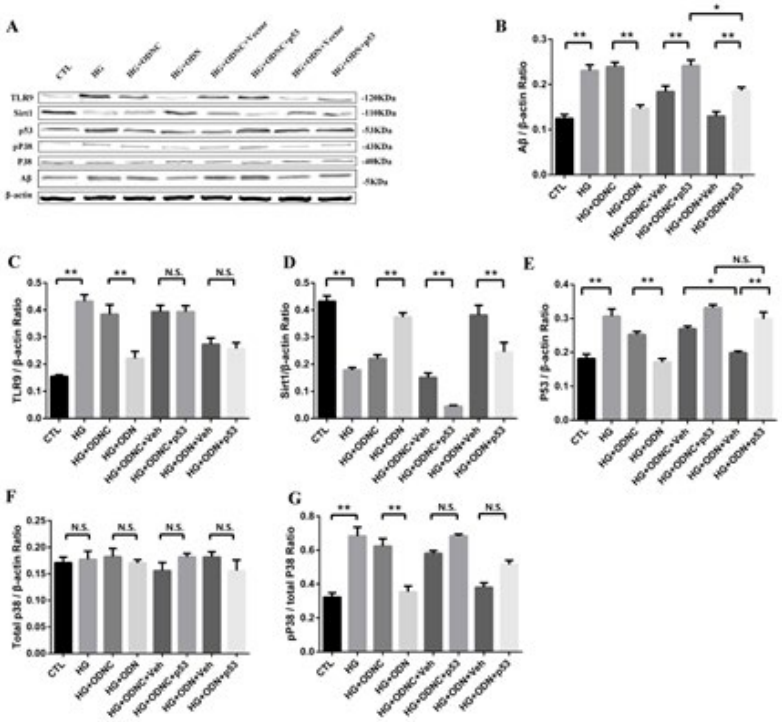

Figure 5. Effect of TLR9 anagonist and p53-overexpression treatments on expression of Aβ, Sirt1 and critical proteins of TLR9 signaling pathway in HT22 cell line incubated with high glucose. (A) Western blotting of Aβ, Sirt1 and critical proteins of TLR9 signaling pathway in HT22 cell line incubated with high glucose. β-actin was used as the loading control. (B-G) Quantification of Aβ, Sirt1 and expressions of TLR9 signaling pathway. Values for the control group were arbitrarily set to a unit of 1. All data were analyzed using a one-way ANOVA followed by Tukey's post hoc tests. *P<0.05, **P<0.01, N.S., not significant. Results were expressed as mean ± SEM (n=6 per group).

apoptosis decreased, compared with ODN2088 Control group, suggesting that hyperglycemia promoted neuronal apoptosis through activation of TLR9. However, ODN2088 could not reverse the apoptotic rate of HT22 cells, which over expressed p53 and were incubated in high glucose environment, indicating that activation of the TLR9/p53 signalling pathway contributed to high glucose induced neuronal apoptosis (Figures 6C and 6D). In addition, the trend of apoptosis was consistent with up evaluation of pro-caspase 3 expression via WB (Figures 6A and 6B).

Discussion

DM has been a serious metabolic disorder with cardiovascular, renal and nervous complications that is widely investigated. More emerging evidence supports that cognitive impairment is associated with DM, and the duration of DM and level of hyperglycemia have been confirmed to be linked to cognitive decline [13,14]. DG is a crucial region of hippocampus which is a functional area of brain involved in encoding, retrieval and discrimination of episodic memories. Compared with circuit of CA1-CA3 area, the memory function of hippocampus is more dependent on DG area [14-18]. Thus, we focused on the alteration of DG area of diabetes. Meanwhile the spatial memory of diabetic mice was damaged in various degrees; we found Aβ was mainly deposited in DG area which is almost consistent with previous studies. In addition to the cognitive dysfunction and abnormalities in Aβ, we also found that high glucose can induce neuronal apoptosis (Figure 6). Our results confirmed that there are many pathogenic mechanisms of DE that can lead to the accumulation of Aβ in extensive areas of hippocampus and cognitive decline, including insulin resistance and abnormal lipid metabolism, hyperglycemia has closer relationship with Aβ deposition in DG area and inferior learning and memory function.

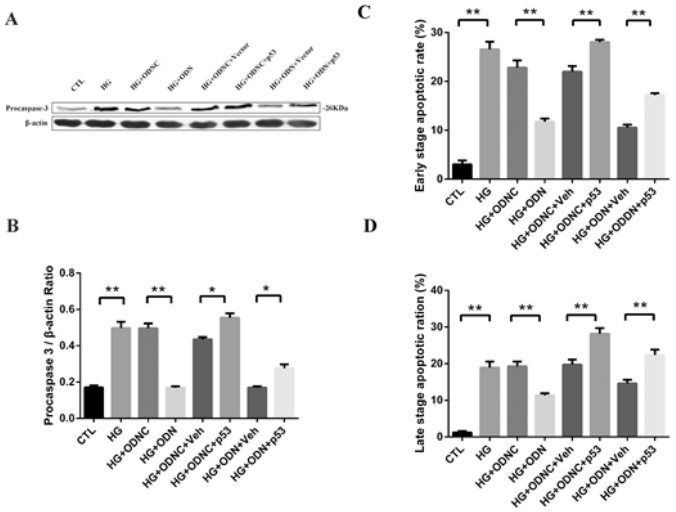

Figure 6. Effect of TLR9 anagonist and p53-overexpression treatments on expression of procaspase3 and cellular apoptosis in HT22 cell line incubated with high glucose. (A) Western blotting of procaspase3 expression in HT22 cell line incubated with high glucose. β-actin was used as the loading control. (B) Quantification of procaspase3 level. Values for the control group were arbitrarily set to a unit of 1. All data were analyzed using a one-way ANOVA followed by Tukey's post hoc tests. *P<0.05, **P<0.01. Results were expressed as mean ± SEM (n=6 per group). (C-D) Flow cytometry of early and late stage apoptosis *in vitro*. All data were analyzed using a one-way ANOVA followed by Dennett's T3 post hoc tests. *P<0.05, **P<0.01. Results were expressed as mean ± SEM (n=6 per group).

As a nicotinamide adenine dinucleotide (NAD+)-dependent protein deacetylase distributed extensively in human brain, the activity or expression of Sirt1 has been proved to be involved in the change of cognitive function of DG area by remodeling or proliferating neurons [8,15,16]. In AD research, Sirt1 has been shown as a neuroprotective role because of its contribution to reduce the Aβ deposition and neuritic plaques in brain. Previous articles have shown that there are ways for Sirt1 to make a difference to Aβ by reducing produce or promoting clearance. These are mainly achieved by regulating the substrates of Sirt1, including a disinterring and metalloproteinase domain containing protein 10 (ADAM10), BACE1, to activate or inhabit the α-secretase, β-secretase or autophagy [10,17-20]. Similar to previous studies, we found the expression of Sirt1 was consisting with the trend of ADAM10, but on the contrary to BACE1 (Figures 4B and 4C). Once Sirt1 was silenced or inhibited *in vivo* or vitro, it was accompanied with the increase of Aβ deposition in DG area and adverse variation of cognitive function. The results indicated that the effects of high glucose on cognition and Aβ deposition were achieved by inhibition of Sirt1 and interference with Sirt1-mediated effects for the α-secretase and β-secretase pathways. Interestingly, the autophagy related proteins remained unchanged when Sirt1 was selectively down regulated (Figures 4D-4G). This indicated that the autophagy engulfment of Aβ was not strongly affected by Sirt1 in type 1 DM.

We have previously demonstrated that TLR9 has the ability to influence cognition through its non-inflammatory signaling pathway. As one of the most critical intracellular receptors involved in regulation of the immune system, TLR9 can specifically recognise some conserved structures in the evolution of microorganisms, including pathogen associated molecular patterns (PAMPs) and host molecules similar to PAMPs, like mitochondrial specific methylated cytosine phosphate guanine sequence, to activate immune response [21-23]. However few studies have investigated the ability of TLR9 on neuronal endoplasmic reticulum (ER) to regulate Aβ metabolism. In our study when knocking out the gene TLR9, the worse learning and memory function of DM mice a nd the more Aβ deposition of DG area in their hippocampus or in neurons cultured in high glucose condition have been reversed, suggesting that TLR9 can act on Aβ to impair cognitive function (Figures 1-3). Furthermore we have found that TLR9 is negatively correlated with Sirt1 and interfered with the regulation of key proteins in Sirt1-mediated α-secretase and β-secretase pathway, which meanwhile leads to the change of cognition and Aβ (Figures 4, 5B and 5D). P53, an oncogene regulator, has been suggested as a possible connection between TLR9 and Sirt1. It can not only be activated by the phosphorylation of P38MAPK (P38 mitogen activated protein kinase), one substrate of TLR9, but also can act on Sirt1. If the nutrition supply is sufficient, wild type p53 can bind to two responsive elements in the Sirt1 promoter to block the transcription of Sirt1 [23-27]. As respected, we found that high glucose has the ability to stimulate TLR9/p38MAPK/p53 signaling pathway to induce neuronal apoptosis and Aβ generation that are mediated by Sirt1 (Figures 2, 5B and 5D). What's worth to mention, as shown in Figures 5C and 5D, selectively up regulating p53 has little effect on TLR9 but significantly inhibit Sirt1, which excludes the inflammatory effects of TLR9 on Sirt1. Therefore, we consider that high glucose can induce Aβ deposition in DG area to impair cognitive dysfunction by TLR9/p53/Sirt1 pathway.

In summary, our study improved our understanding of DE and confirmed that the TLR9/p53 signalling pathway negatively regulated Sirt1 to accelerate Aβ deposition in brain and cognitive impairment. These results not only provided mechanistic evidence for Aβ deposition in the brain but also supported the hypothesis that high glucose was an independent risk factor for cognitive damage. The function of immune receptor TLR9 on the parenchymal cell in the induction of Aβ and excessive phosphorylation of Tau through the non-immune signalling pathway may provide new insights into the diagnosis and treatment of DE.

Conclusion

Ethics approval and consent to participate

All animal experimental operations were performed in the daytime, strictly according to the Guide for the Care and Use of Laboratory Animals of the National Institutes of Health (NIH Publications NO.8023, revised 1978).

The study was approved by the Animal Ethics Committee of The First Affiliated Hospital of Chongqing Medical University. All animal experiments complied with the ARRIVE guidelines.

Consent for Publication

Not applicable.

Availability of Data

The raw data required to reproduce these findings cannot be shared at this time as the data also forms part of an ongoing study.

Conflict of Interest

None.

Funding

Our work was supported by Chongqing Natural Science Foundation (cstc2018jcyjAX0762); National Natural Science Foundation of China (No. 81901424)National Natural Science Foundation of China (No. 81801385).

Authors' Contributions

Yue Sun, Qian Xiao contributed to the conception of the study; Yue Sun performed the experiment; Yue Sun, Shiyu Zhu contributed significantly to analysis and manuscript preparation; Yue Sun, Shiyu Zhu, Qian Xiao performed the data analyses and wrote the manuscript; Jinliang Chen, Jing Zhou, Yuxing Zhao、Luo Cheng, Lv Qiong, Kexiang Zhao, Yuan Gao, Di Wang helped perform the analysis with constructive discussions.

Acknowledgement

Thanks are due to Shiyu Zhu, Jinliang Chen, Jing Zhou, Yuxing Zhao, Luo Cheng for assistance with the experiments and to Qian Xiao, Kexiang Zhao for valuable discussion and funding support.

References

1. Reske-Nielsen, E and Lundbulk K. “Pathological changes in the central and peripheral nervous system of young long-term diabetics”. Diabetologia 1(1966):233-241.
2. Juliette, J, L Thomas, JE Parisi and Peter C Butler, et al. “Increased risk of type 2 diabetes in alzheimer disease”. Diabetes 53(2004):1206-1222.
3. TD, Heijer, SE Vermeer, EJV Dijk and MMB Breteler, et al. “Type 2 diabetes and atrophy of medial temporal lobe structures on brain MRI”. Diabetologia 46(2003):1604-1610.
4. Antonio, Currais, Marguerite Prior, David Lo and Pamela Maher, et al. “Diabetes exacerbates amyloid and neurovascular pathology in aging-accelerated mice”. Aging Cell 11(2013): 1017–1026.
5. Haass, C and Selkoe DJ. “Soluble protein oligomers in neurodegeneration: Lessons from the Alzheimer's amyloid beta-peptide”. Nat Rev Mol Cell Biol 8(2007):101-12.
6. Takeda, S, Sato N, Uchio-Yamada K and Ryuichi Morishita, et al. “Diabetes-accelerated memory dysfunction via cerebrovascular inflammation and Aβ deposition in an Alzheimer mouse model with diabetes”. Proc Natl Acad Sci U S A 107(2010):7036-41.
7. Joshua, A, Sonnen, Eric B and Larson et al. “Different patterns of cerebral injury in dementia with or without diabetes”. Arch Neurol 66(2009):315-322.
8. Christopher, L, Brooks and Wei Gu. “How does SIRT1 affect metabolism, senescence and cancer?.” Nat Rev Cancer, 9(2009):123-128.
9. Wang, W, Sun W, Cheng Y and Lu Cai, et al. “Role of sirtuin-1 in diabetic nephropathy”. J Mol Med 97(2019):291-309.
10. Wencel, PL, Lukiw WJ, Strosznajder JB and Strosznajder RP. “Inhibition of poly(adp-ribose) polymerase-1 enhances gene expression of selected sirtuins and app cleaving enzymes in amyloid beta cytotoxicity”.Mol Neurobiol 55(2017):4612-4623.
11. Sun, Y, Xiao Q, Luo C and Zhao Y, et al. “High-glucose induces tau hyper phosphorylation through activation of TLR9-P38MAPK pathway”. Exp Cell Res 359(2017):312-318
12. Naoyuki, Sato and Ryuichi Morishita. “Brain alterations and clinical symptoms of dementia in diabetes: aβ/tau-dependent and independent mechanisms”. Front Endocrinol (Lausanne) 5(2014):143.
13. Feiyan, Fan, Tao Liu, Xin Wang and Jianfang Fu, et al. “CIC-3 expression and its association with hyperglycemia induced ht22 hippocampal neuronal cell apoptosis”. J Diabetes Res 2016(2016): 2984380.
14. Elena, P Moreno-Jiménez , Miguel Flor-García and Julia Terreros-Roncal, et al. “Adult hippocampal neurogenesis is abundant in neurologically healthy subjects and drops sharply in patients with alzheimer's disease”. Nat Med 25(2019):554-560
15. Alan, Hinojosa-Godinez and Luis F Jave-Suarez. “Melatonin modifies SOX2 + cell proliferation in dentate gyrus and modulates SIRT1 and MECP2 in long-term sleep deprivation”. Neural Regen Res 14(2019):1787-1795.
16. Diankun, Yu , Damek R and Homiack. “BK channel deacetylation by sirt1 in dentate gyrus regulates anxiety and response to stress”. Commun Biol 1(2018):82.
17. Yuta, Senzai. “Function of local circuits in the hippocampal dentate gyrus-CA3 system”. Neurosci Res 140(2019):43-52.
18. Thomas, Hainmueller and Marlene Bartos. “Dentate gyrus circuits for encoding, retrieval and discrimination of episodic memories”. Nat Rev Neurosci 21(2020):153-168.
19. Yanqing, Wu , Libing Ye and Yuan Yuan. “Autophagy activation is associated with neuro protection in diabetes-associated cognitive decline”. Aging Dis 10(2019):1233-1245.
20. Hung, SY, Huang WP, Liou HC and Wen-Mei Fu, et al. “Autophagy protects neuron from Aβ-induced cytotoxicity”. Autophagy 5(2009):502-10
21. Shintani, Y, Kapoor A, Kaneko M and Ken Suzuki, et al. “TLR9 mediates cellular protection by modulating energy metabolism in cardiomyocytes and neurons”. Proc Natl Acad Sci USA 110(2013):5109-14.
22. Zhang, Q and Itagaki K. “Mitochondrial Dna is released by shock and activates neutrophils via p38 map kinase”. Shock 34(2010):55-9.
23. Gu, X, Wu G, Yao Y and Zeng J, et al. “Intratracheal administration of mitochondrial DNA directly provokes lung inflammation through the TLR9–p38 MAPK pathway”. Free Radic Biol Med 83(2015):149-58.
24. Nemoto, S, Fergusson MM and Finkel T. “Nutrient availability regulates sirt1 through a forkhead-dependent pathway”. Science

306(2004):2105-8

25. Herskovits, AZ and Guarente L. “SIRT1 in neurodevelopment and brain senescence”.Neuron 81(2014):471-83
26. Gonfloni, S, Iannizzotto V, Maiani E and Marc Diederich, et al. “P53 and Sirt1: Routes of metabolism and genome stability”. Biochem Pharmacol 92(2014):149-56.
27. She, QB, Chen N and Dong Z. “ERKs and p38 kinase phosphorylate p53 protein at serine 15 in response to UV radiation”. J Biol Chem 275(2000): 20444−20449.

How to cite this article: Sun, Yue, Shiyu Zhu, Jinliang Chen and Yuxing Zhao, et al. "Sirt1 Mediated High-Glucose Induced Aβ Deposition and Cognitive Impairment through Activation of the TLR9/P53 Pathway." *J Neurol Disord* 10(2022): 264